

Solid–Liquid Equilibria for the CO₂ + R143a and N₂O + R143a Systems

Giovanni Di Nicola · Matteo Moglie ·
Giulio Santori · Roman Stryjek

Received: 25 September 2008 / Accepted: 29 June 2009 / Published online: 14 July 2009
© Springer Science+Business Media, LLC 2009

Abstract A recently built experimental setup for determination of solid–liquid equilibria was slightly modified. The action taken on the existing system focused on correcting the drawbacks of the cooling system. In this version of the setup, a direct liquid nitrogen supply was preferred. By means of the modified apparatus, solid–liquid equilibria of the CO₂ + R143a and N₂O + R143a binary systems were studied. The triple point of R143a was measured to check the reliability of the modified apparatus, revealing good consistency with the literature. The system's behavior was measured down to temperatures of 148 K. The results obtained for the mixtures were interpreted by means of the Schröder equation.

Keywords Carbon dioxide · Cascade units · Eutectic · Nitrous oxide · Refrigerants · Solid–liquid equilibria

1 Introduction

As already discussed in previous papers [1–3], solid–liquid equilibria (SLE) play an important role in refrigeration, for the estimation of the lowest temperature at which a blend can be used as a refrigerant fluid. This information is particularly useful for very low-temperature applications, i.e., cascade refrigeration units, where temperatures down to 150 K are commonly reached. In addition, SLE provide theoretical

G. Di Nicola (✉) · M. Moglie · G. Santori
Dipartimento di Energetica, Università Politecnica delle Marche, Ancona, Italy
e-mail: g.dinicola@univpm.it

R. Stryjek
Institute of Physical Chemistry, Polish Academy of Sciences, Warsaw, Poland

information on the real behavior of studied systems at low temperatures in terms of the eutectic composition and activity coefficients.

Most SLE measurements enable visual observation of the disappearance of the last amount of solid phase and relatively easy temperature control [4]. The experimental temperature ranges usually spans from 200 K to 400 K. Since the systems under study could be expected to have temperature ranges from 200 K down to about 155 K, we decided that it would be technically more feasible to use a method with no visual observation of phase behavior.

The setup specifically built for this purpose showed some limitations in terms of drainage of condensation, system cut-out problems, sensitivity of the system to atmospheric conditions, high wastage of nitrogen, system inertia, and velocity adjustment problems. Given all these drawbacks, action was taken mainly on the cooling system, for which a direct nitrogen supply was preferred.

In previous studies [1–3], using the first version of the experimental setup, together with the properties of the $\text{CO}_2 + \text{N}_2\text{O}$ binary system [2], SLE of $\text{CO}_2 +$ and $\text{N}_2\text{O} +$ four different HFCs (R125, R32, R134a, and R152a) were explored. The main motivation for these binaries lies in the possibility to combine the advantages of natural fluids in terms of low environmental impact (i.e., $\text{GWP} = 1$ for CO_2 and $\text{GWP} = 310$ for N_2O , which can be considered low if compared with HFCs) together with those of HFCs in terms of performance and of the possibility to extend the temperature application limit.

In this article, using the modified experimental setup, SLE of the $\text{CO}_2 + \text{R143a}$ and $\text{N}_2\text{O} + \text{R143a}$ binary systems were studied. No information on the SLE of these binary systems was available in the literature.

2 Description of the Apparatus

2.1 Measurement Cell

The experimental setup is shown in Fig. 1. The measuring cell (1), with a volume of approximately 47 cm^3 , was made out of a stainless steel cylinder with a cover welded to the body. Before welding, a stirrer (2) consisting of a stainless steel rod having a rounded end with two steel blades welded onto it was placed in the cell. The stirrer was kept in a perfectly vertical position by means of conical seats created on the raised bottom of the cell and on the underside of the cover so as to contain the rounded ends of the rod. Two holes were drilled in the cover, and a stainless steel tube with a diameter of 4 mm was inserted through and welded to the hole on the left for charging the cell with gas, while the hole on the right, which was 6.25 mm in diameter, was used to house the thermometer (3), the end of which was inserted down to approximately 2.7 cm from the bottom of the cell. The purpose of the stirrer was to prevent any premature stratification of the fluids comprising the various mixtures, while also assuring greater homogeneity during the liquefaction and crystallization of the mixture. The stirrer inside the cell was turned by a magnet, which drives the plate welded onto the lower end of the rod. The magnet was housed in a seat made of brass, which was connected to the shaft of an electric engine driving the rotation of the magnet and thus also of

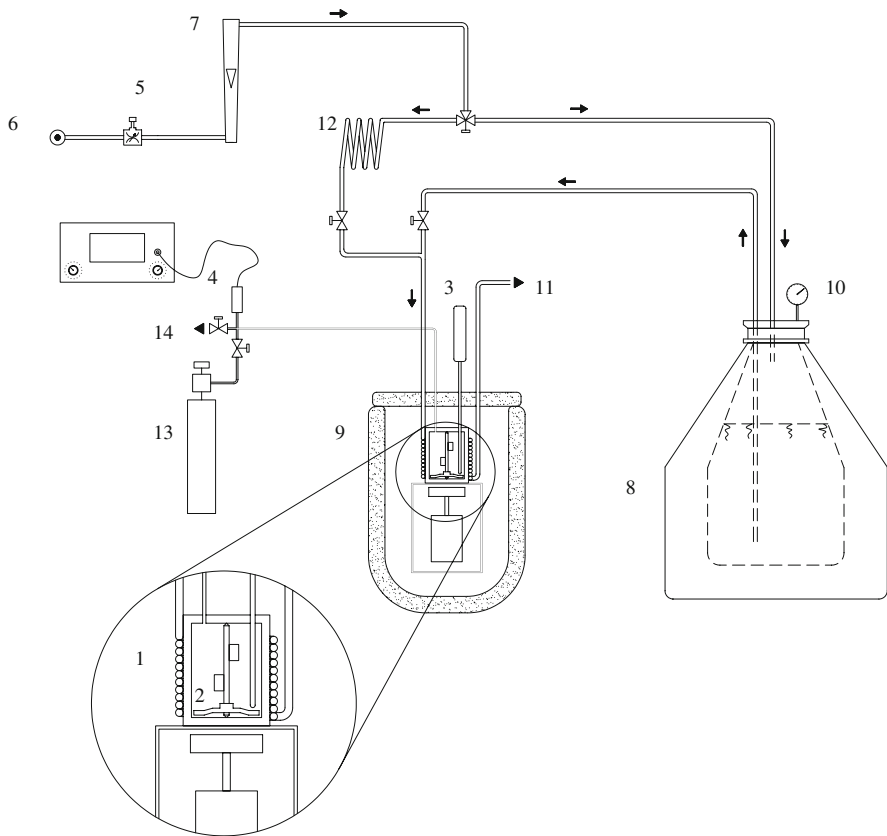


Fig. 1 Schematic illustration of the apparatus: 1 Measurement cell, 2 Stirrer, 3 Platinum resistance thermometer, 4 Pressure transducer, 5 Mass flow controller, 6 Dry air supplier, 7 Rotameter, 8 Liquid nitrogen tank, 9 Dewar containing the measurement cell, 10 Liquid nitrogen dewar manometer, 11 Nitrogen outlet, 12 External heating coil, 13 Charging bottle, 14 Vacuum pump system

the stirrer inside the cell. An absolute pressure transducer (HBM, Mod. P8A) (4) was installed in the charging tube.

A mass flow control (5) was installed upstream from the dehumidifier; a needle valve with a shutter was used to adjust the flow rate coming from the dry air supplier (6), as measured by means of the pressure difference reading on a pressure gauge alongside it. The airflow was also measured by a rotameter (7).

2.2 Cooling System

The previously adopted system involved indirect use of liquid nitrogen, which was poured into a Dewar flask provided at the base of the circuit. The new apparatus includes a system for drawing the liquid nitrogen directly from its insulated tank with the aid of compressed air; the carrier fluid circulating in the circuit is thus the refrigerant fluid itself, instead of passing through an exchange with air.

The cooling system as a whole is thus reduced to four functional parts: the compressed air circuit that creates a positive pressure in the liquid nitrogen tank, the thermally insulated liquid nitrogen tank (8), the hose connecting the tank to the circuit, completes with a faucet, and the copper coil that surrounds and exchanges heat with the cell. The core element in the whole cooling system is the copper coil surrounding the measuring cell; through its contact surface, the coil removes heat by means of the refrigerant fluid flowing inside it. The copper coil and cell are placed together inside a Dewar flask (9) so as to further isolate them from the outside environment. The system as a whole is suitably covered with neoprene foam for thermal insulation. The flexible connection hoses for the liquid nitrogen flowing from the insulated container, driven by the difference in pressure, are made of a silicone material that can withstand even the very low temperatures of this refrigerant fluid.

The operation of the system as a whole can be divided into two separate circuits and consequently two operating modes: a cooling system and a heating system. When the system is used in the cooling mode, the compressed air (after passing through suitable dehumidifier filters) is delivered to the liquid nitrogen tank, which is thus placed under a positive pressure. Inside the tank, a PVC hose draws the refrigerant fluid from the bottom, which begins to flow through the circuit as soon as the pressure in the tank, controlled by a manometer (10), is sufficient to overcome the load losses produced by the circuit. After the first few moments, a steady state is reached and the liquid nitrogen flows through the circuit, rapidly cooling all of its surfaces to a very low temperature. The refrigerant fluid passes first through the silicone capillary, then through the copper piping, exchanging heat with the measuring cell by evaporation as it moves through the coil, and finally flows out from the nitrogen outlet (11). In this cooling configuration, the nitrogen valve remains open and the heating circuit valve remains closed.

Conversely, when the system is operated in the heating mode, the dehumidified compressed air circuit is connected directly to the measuring cell's circuit and, in this case, the air acts as a carrier fluid and warms the cell, which is at a very low temperature by the end of a measurement procedure. In this configuration, the nitrogen inlet valve remains closed. An external copper coil (12) has also been provided: this can be heated by the operator to speed up the warming of the measuring cell.

2.3 Previous Apparatus Drawbacks

The action taken on the previous system focused on correcting and, where possible, eliminating the known drawbacks of the previous system.

1. The previous system involved the need to periodically drain off the condensation (mainly liquid air) accumulating in the system, which was responsible not only for a pointless waste of cooling capacity, but also for a major risk of falsifying the measurements if care was not taken to drain the condensation far from the measurement interval because, each time the condensation was drained off, there was a temporary increase in the temperature of the cell, with a consequent transient disruption of the normal trend of the cooling curve.

2. System cut-out problems: despite the dehumidifier filters upstream from the compressed air circuit, it was not unusual for the circuit to cut out due to ice forming during the cooling cycle, with an obvious fallout on the measurement underway, which had to be repeated after re-warming and unclogging the system.
3. Sensitivity of the system to atmospheric conditions: using atmospheric air as a carrier fluid (duly dehumidified by the filters provided), the proper operation, the cooling rate, and consequently also the measurements obtained tended to depend to some degree on environmental climatic conditions. The system could not guarantee a constant behavior for the various seasons of the year and for different characteristics of the ambient air.
4. Major wastage of nitrogen: the old system involved the transfer of liquid nitrogen from the insulated bottles to the Dewar flask. In addition to a considerable hazard to the operators, this meant high consumption of the refrigerant fluid because it tended to evaporate rapidly and in considerable quantities, especially in the initial phase when the Dewar flask was still at ambient temperature.
5. System inertia: the liquid nitrogen was previously used to cool the system's carrier fluid proper as it passed through the copper coils. This meant a certain degree of inertia in the system as a whole, which took time to respond to any adjustments.
6. Velocity adjustment problems: the operator had to adjust the cooling rate by changing the flow rate of the compressed air in the circuit. The main disadvantage of this method was an increase in the density of the carrier fluid as the temperatures fell, and the consequent need for continual flow rate corrections by the operator in an attempt to keep it as constant as possible.

Given all these drawbacks, a direct nitrogen supply was preferred.

2.4 Temperature Measuring Systems

To monitor the temperatures, the apparatus was equipped with one thermoresistance placed in the measuring cell. The system parameters and the efficiency of the coil immersed in the liquid nitrogen were assessed using thermocouples at specific points on the copper tube. The platinum resistance thermometer used in the apparatus (100 Ω , Minco, Mod. S7929) was calibrated by comparison with a 25 Ω platinum resistance thermometer (Hart Scientific, Mod. 5680 SN1083).

3 Experimental Procedure and Uncertainties

3.1 Experimental Procedure

The charging procedure consisted of the following steps: the bottle containing the refrigerant gas (13) was weighed on the electronic balance (the uncertainty of which is 0.5 mg); then the bottle was connected to the apparatus and to the vacuum pump (14) (Vacuubrand, Mod. RZ2), a vacuum was created inside the measuring cell and the charging tube as recorded on the vacuum pump gauge (Galileo, Mod. OG510); then the fluid was charged by opening the valve on the gas bottle; the temperature of

the cell was brought down by a flow of liquid nitrogen so as to insert the whole mass in the cell, leaving as little as possible in the charging tube; a suitable time interval was allowed so that the pressure, being lowered by the temperature reduction, could drop to below atmospheric pressure, then the on/off valve was closed; and the gas bottle was disconnected and weighed again to establish the actual mass charged in the cell.

The coil with liquid nitrogen was wrapped around the measuring cell. Monitoring the time dependence of the temperature, a cooling curve was obtained for each sample concentration. While the change of phase occurs, the heat removed by cooling is compensated for by the latent heat of the phase change, showing a change of slope in the temperature trend. The arrest in cooling during solidification allows the melting point of the material to be identified on the time–temperature curve. The melting points can then be plotted versus the composition to give a phase diagram.

3.2 Uncertainties

All the uncertainties were calculated using the law of error propagation, as reported elsewhere [1]. Here, the previously reported results will be briefly summarized.

The total uncertainty of the mass of sample mixture was less than 0.01 g. The uncertainty in composition measurements was estimated to be always less than 0.005 in mole fraction. The total uncertainty for the temperature, using the law of error propagation, was calculated to be less than 0.023 K.

Since the measured vapor-pressure data were not accurately measured at very low temperatures within the declared precision of the used instrument (the pressure values were acquired by an absolute pressure transducer HBM, Mod. P8A, and the global uncertainty of the pressure measurements was estimated to be less than 3 kPa), the vapor-pressure data were not reported in the present paper.

4 Experimental Results

As concerns the pure fluids, since data are already available in the literature on their triple point, we took the test measurements to confirm these data and thereby verify the functional efficiency and fine adjustment of the apparatus we had modified. Regarding the mixtures with constituents considered, there are no data on the SLE in the literature, so the present study covers new ground and the data we obtained can be used as the starting point for future studies.

4.1 Chemicals

Carbon dioxide and nitrous oxide were supplied by Sol SpA. Their purity was checked by gas chromatography, using a thermal conductivity detector, and was found to be 99.99 mass % for both fluids, basing all estimations on an area response. R143a was donated by Ausimont SpA; its purity was found to be 99.9 mass % on an area response.

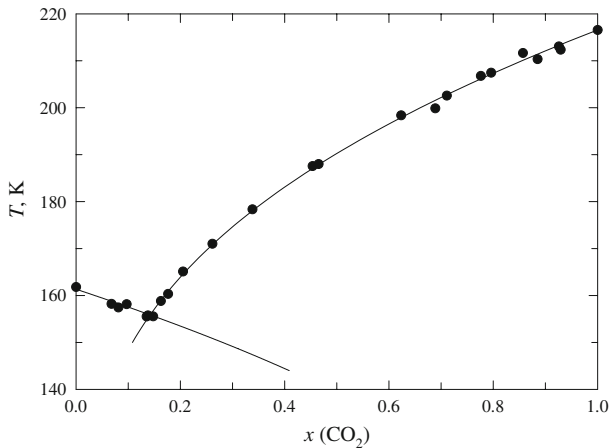


Fig. 2 SLE for the $\text{CO}_2 + \text{R143a}$ system: *black symbols* denote the experimental points while the *lines* denote the Schröder equation

4.2 Pure Fluids

For carbon dioxide and nitrous oxide, results are presented elsewhere [1,2]. The tests conducted showed that a faster cooling rate coincided with a greater supercooling effect. The cooling rate that seemed to guarantee the greatest repeatability of the results was approximately $-0.01 \text{ K} \cdot \text{s}^{-1}$, corresponding to an air flow rate of approximately $0.17 \text{ dm}^3 \cdot \text{s}^{-1}$. For both pure fluids a metastable phase appeared. Triple-point measurements showed good agreement with literature sources, both in terms of temperature and pressure [1,2].

For R143a, the metastable phase did not appear during the measurements, and only a change of slope was evident in the temperature–time diagram. However, the triple-point temperature was clearly evident at a temperature of 161.4 K, in agreement with literature results [5] that report a triple point of 161.34 K.

4.3 Results for Mixtures

Measurements were taken using different concentrations of the two components, obtaining a satisfactory number of points, which were then recorded on a concentration/temperature graph ($T - x$). Moreover, conducting several tests on the same sample, we noted that we obtained better, more reliable results by switching off the stirrer before reaching the triple-point temperature. We consequently decided to turn off the stirrer at least about 30 K (a value suggested by experience) from the triple point.

The $T - x$ measurements for the two systems considered ($\text{CO}_2 + \text{R143a}$ and $\text{N}_2\text{O} + \text{R143a}$, respectively) are given in Figs. 2 and 3. The results are also summarized in Table 1. From the $T - x$ data, it is evident that both systems form eutectics ($x_1 = 0.14$ at $T = 156 \text{ K}$ for $\text{CO}_2 + \text{R143a}$ and $x_1 = 0.36$ at $T = 147 \text{ K}$ for $\text{N}_2\text{O} + \text{R143a}$).

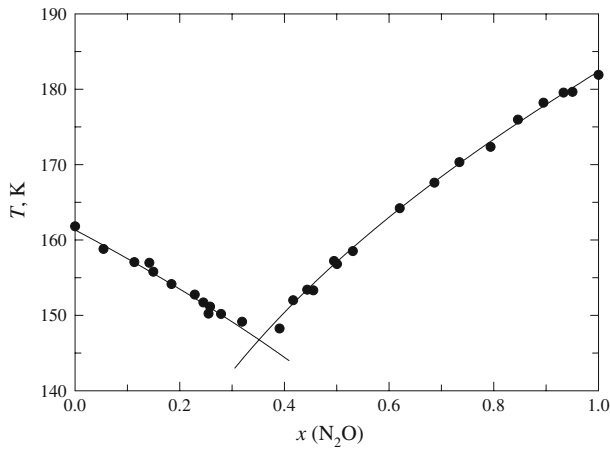


Fig. 3 SLE for the N_2O + R143a system: *black symbols* denote the experimental points while the *lines* denote the Schröder equation

Since the results were obtained while maintaining a constant cooling rate of approximately $-0.01 \text{ K} \cdot \text{s}^{-1}$ and considering that no metastable state (supercooling) was evident during the mixture measurements, the experimental results were not corrected by the Rossini method [6].

As both systems formed eutectics, the solubility of the solid solute in the solvent (here, R143a) can be described by the Schröder equation [7], which disregarding any difference between the heat capacity of the subcooled liquid solute and solid solute takes the following form:

$$\ln \gamma_2 x_2 = -\frac{\Delta h_m}{RT} \left(1 - \frac{T}{T_m} \right) \quad (1)$$

where the subscript 2 denotes the solute and the subscript m denotes the property at the melting point. It was assumed as a first approximation that the solute's activity coefficient, $\gamma_2 = 1$; this means that we can write

$$\ln x_2 = -\frac{\Delta h_m}{RT} \left(1 - \frac{T}{T_m} \right) \quad (2)$$

This simplification leads to the consideration that the solubility of the solid solute is independent of the solvent as far as the assumptions hold. The enthalpies at the melting point (Δh_m) were assumed to be $9020 \text{ J} \cdot \text{mol}^{-1}$ [8], $6540 \text{ J} \cdot \text{mol}^{-1}$ [8], and $5853 \text{ J} \cdot \text{mol}^{-1}$ [5], for CO_2 , N_2O , and R143a, respectively.

The course of the liquidus calculated with the Schröder equation is included in Figs. 2 and 3. Both systems followed the Schröder equation.

Table 1 $T - x$ Measurements for the $\text{CO}_2 + \text{R143a}$ and $\text{N}_2\text{O} + \text{R143a}$ binary systems

$\text{CO}_2(1) + \text{R143a}(2)$		$\text{N}_2\text{O}(1) + \text{R143a}(2)$	
x_1	T (K)	x_1	T (K)
0.000	161.8	0.000	161.8
0.068	158.2	0.054	158.8
0.081	157.5	0.113	157.1
0.097	158.2	0.142	157.0
0.135	155.5	0.150	155.8
0.138	155.8	0.184	154.2
0.148	155.6	0.229	152.8
0.163	158.8	0.245	151.7
0.176	160.3	0.255	150.2
0.205	165.1	0.258	151.2
0.261	171.0	0.279	150.2
0.338	178.4	0.319	149.2
0.453	187.6	0.391	148.3
0.465	188.0	0.417	152.0
0.623	198.4	0.444	153.4
0.689	199.9	0.455	153.3
0.711	202.6	0.495	157.2
0.776	206.8	0.501	156.8
0.796	207.5	0.531	158.5
0.857	211.7	0.620	164.2
0.885	210.4	0.687	167.6
0.926	213.1	0.734	170.3
0.929	212.4	0.794	172.4
1.000	216.6	0.846	176.0
		0.895	178.2
		0.933	179.6
		0.950	179.7
		1.000	181.9

5 Conclusion

In this article, a modified experimental setup for SLE exploration is presented. The SLE behavior of $\text{CO}_2 + \text{R143a}$ and $\text{N}_2\text{O} + \text{R143a}$ were measured down to temperatures of 147 K.

When the new setup is used in the cooling mode, the liquid nitrogen flows through the circuit, rapidly cooling all of its surfaces to a very low temperature. When it is used in the heating mode, the dehumidified compressed air acts as a carrier fluid and warms the cell.

The triple points of the R143a pure fluid was measured to check the reliability of the new apparatus, revealing good consistency with the literature. The $\text{CO}_2 + \text{R143a}$ and $\text{N}_2\text{O} + \text{R143a}$ systems showed the presence of an eutectic and generally good agreement with Schröder equation predictions. No other SLE experimental data were found in the open literature for these specific binary systems.

References

1. G. Di Nicola, G. Giuliani, F. Polonara, R. Stryjek, *J. Chem. Eng. Data* **51**, 2209 (2006)
2. G. Di Nicola, G. Giuliani, F. Polonara, R. Stryjek, *Fluid Phase Equilib.* **256**, 86 (2007)
3. G. Di Nicola, G. Giuliani, F. Polonara, G. Santori, R. Stryjek, *J. Chem. Eng. Data* **52**, 2451 (2007)
4. K. Fukné-Kokot, A. König, Ž. Knez, M. Škerget, *Fluid Phase Equilib.* **173**, 297 (2000)
5. J.W. Magee, *Int. J. Thermophys.* **19**, 1397 (1998)
6. B.J. Mair, J.A.R. Glasgow, F.D. Rossini, *J. Res. Nat. Bur. Standards* **26**, 591 (1941)
7. I. Schröder, *Z. Phys. Chem.* **11**, 449 (1893)
8. D.R. Lide, H.V. Kehiaian, *CRC Handbook of Thermophysical and Thermochemical Data* (CRC Press, Inc., Boca Raton, Florida, 1994)